Pavlos-Antonios Sampanis, a Food Scientist – Agronomist, recently graduated from the Agricultural University of Athens, Greece, with a degree of a five years program in Food Science and Human Nutrition. His thesis work was entitled *Analysis of shell egg pasteurization using Computational Fluid Dynamics*. Always eager to learn and acquire experience in the field of food science. Working also and specialized in viticulture.

IFTPS 2023 Annual Meeting February 28 - March 2, 2023, New Orleans, LA

Analysis of shell egg pasteurization using Computational Fluid Dynamics

Pavlos-Antonios Sampanis[1,*], Stelios M. Chatzidakis[1], Nikolaos G. Stoforos[1]

[1] Department of Food Science and Human Nutrition, Agricultural University of Athens, Athens, Greece
* pavlos.sabanis@gmail.com

Objectives

- Development of 3D heat transfer model for shell egg pasteurization process
- Validation of the theoretical model against experimental data
- Prediction of the time-temperature profile and critical point location
- Estimation of the pasteurization efficiency of the process, including heating and cooling
- Estimation of the nutrient degradation during pasteurization

The Egg

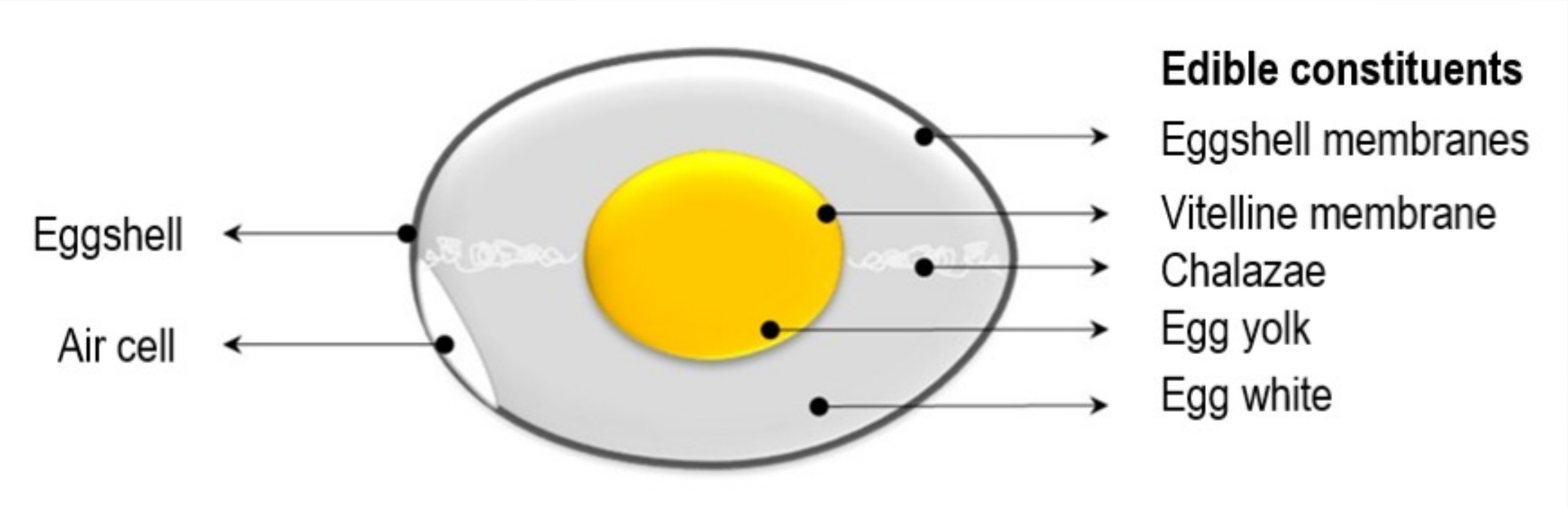

Figure 1. The egg and its structural components.

Nutrient rich, easily digestible and affordable. But also, perishable and potentially hazardous food.

Outbreaks

Salmonella outbreak in Sweden linked to eggs

By Joe Whitworth on January 19, 2023

More than 20 people have fallen ill in Sweden with the source of their infections suspected to be eggs.

Multi-country outbreak of *Salmonella* Enteritidis sequence type (ST)11 infections linked to eggs and egg products – 8 February 2022

European Centre for Disease Prevention and Control, European Food Safety Authority

First published: 10 February 2022 | https://doi.org/10.2903/sp.efsa.2022.EN-7180 | Citations: 1

Egg pasteurization

FDA has recommended thermal treatment for a 5-log reduction of *Salmonella enterica* ($D_{60^\circ C}$ = 0.17 min, *z* value = 4.1°C).

Thermal pasteurization remains the principal method to ensure the safety of eggs and egg products. However, pasteurization process occurs in only 1% of the shell eggs available in the market.

Egg pasteurization

Methods of industrial egg pasteurization include:

- Water immersion (Water-bath at 57°C for 25 min)
- Hot-air pasteurization
- Humid air pasteurization
- Microwave egg pasteurization

The optimization of the process is necessary to ensure food safety, without significant quality degradation.

Computational Fluid Dynamics (CFD)

Computational Fluid Dynamics, usually abbreviated as CFD, is a branch of fluid mechanics that uses numerical analysis and algorithms to solve and analyze problems that involve fluid flows.

(https://en.wikipedia.org/wiki/Computational_fluid_dynamics)

Partial differential equations describing momentum, heat, and mass transfer coupled with equilibrium and kinetic equations, which usually form a model for a processing operation, can be solved easily with today’s computing capabilities.

Computational Fluid Dynamics (CFD)

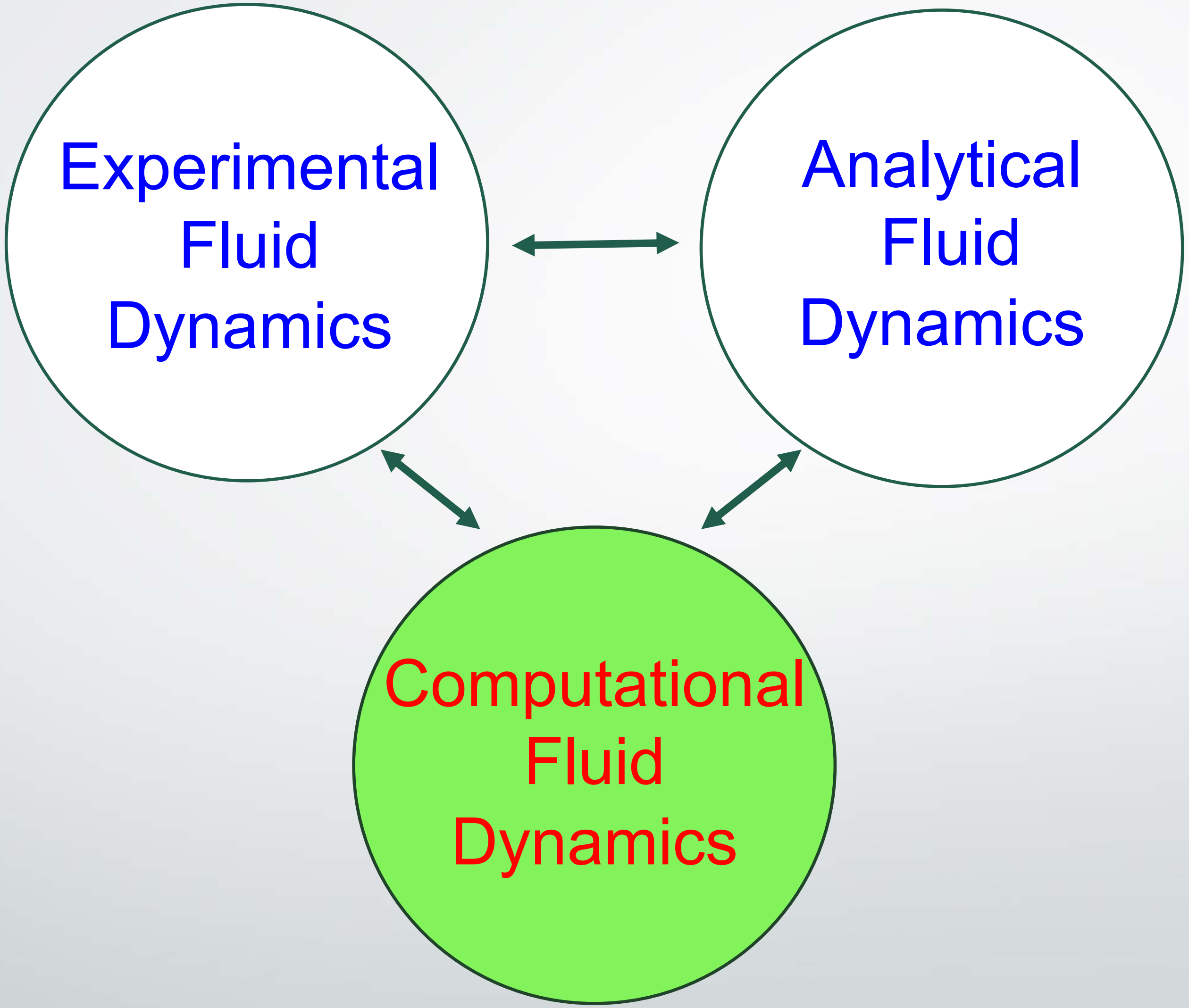

Computational Fluid Dynamics (CFD)

A number of common steps are always followed in the solution of a problem with CFD:

- The geometry of the system is defined
- The computational domain is divided into cells
- The initial and boundary conditions are defined
- The physical model is defined
- The solution is obtained at each nodal point
- The post-processing of the results is used for the analysis and visualization of the solution
- Solution verification (experimental)

Equation of energy conservation

$$\rho c_p \left(\frac{\partial T}{\partial t} + v \frac{\partial T}{\partial r} + u \frac{\partial T}{\partial z} \right) = k \left\{ \frac{1}{r} \frac{\partial}{\partial r} \left(r \frac{\partial T}{\partial r} \right) + \frac{\partial^2 T}{\partial z^2} \right\}$$

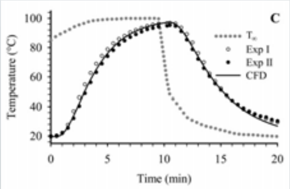

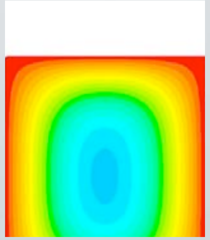

CFD in food processing

CFD applications in processing operations in the food industry:

- Baking
- Drying
- Mixing
- Refrigeration
- Heat exchangers
- Pasteurization
- Sterilization (commercial sterilization)

CFD applications

- Thermal processing of table olives in brine

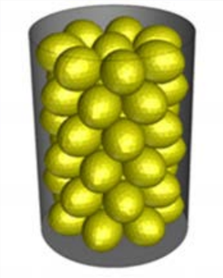

- Thermal processing of still cans filled with peach halves in sugar syrup

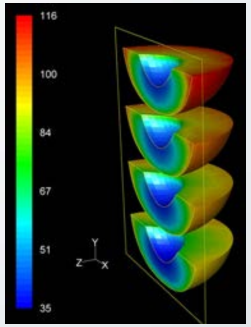

- Quality evaluation in conduction heating canned foods

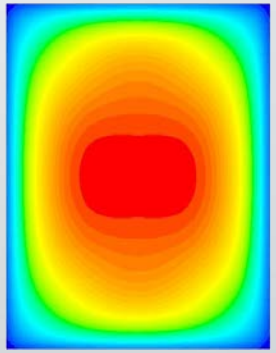

- Hot fill processes for tomato products

Materials and Methods

CFD model design

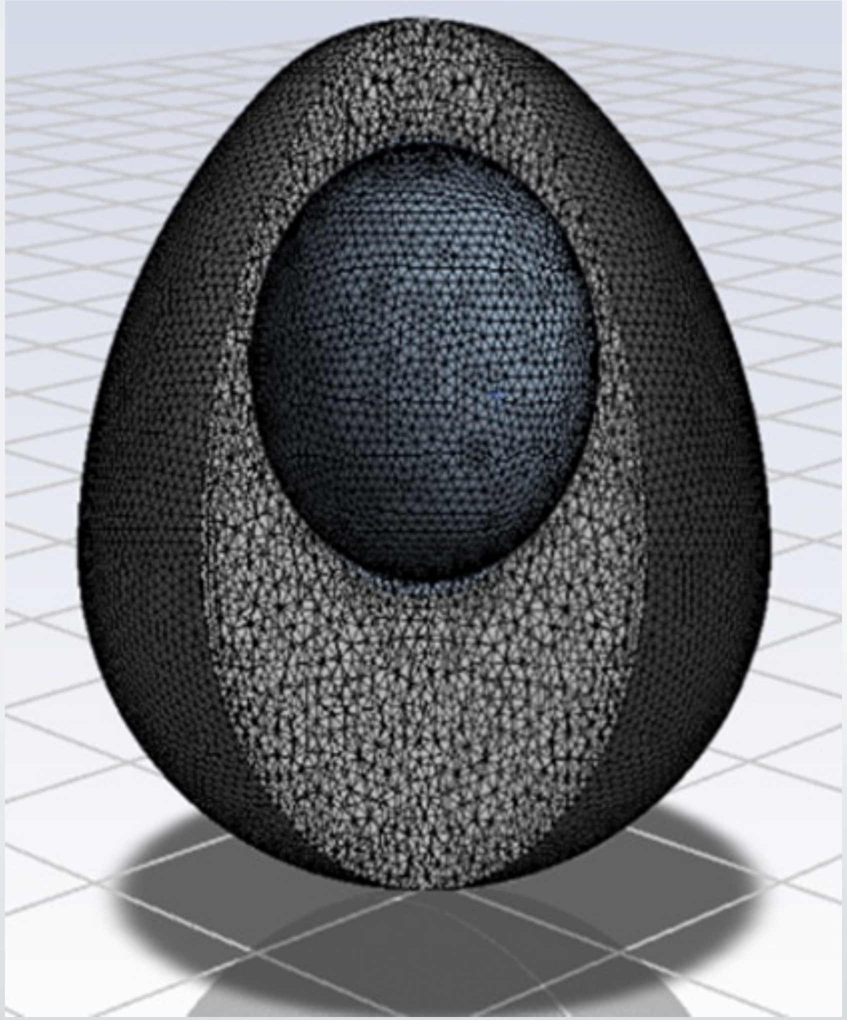

Figure 2. Generated mesh imaging.

Model assumptions

- The yolk and egg white are homogenous
- The initial temperature of the eggs was considered uniform
- The natural convectional flow of fluid was assumed in the gravitational direction
- The effect of eggshell thickness and % of air cell on heat transfer was considered minimal

CFD model geometry

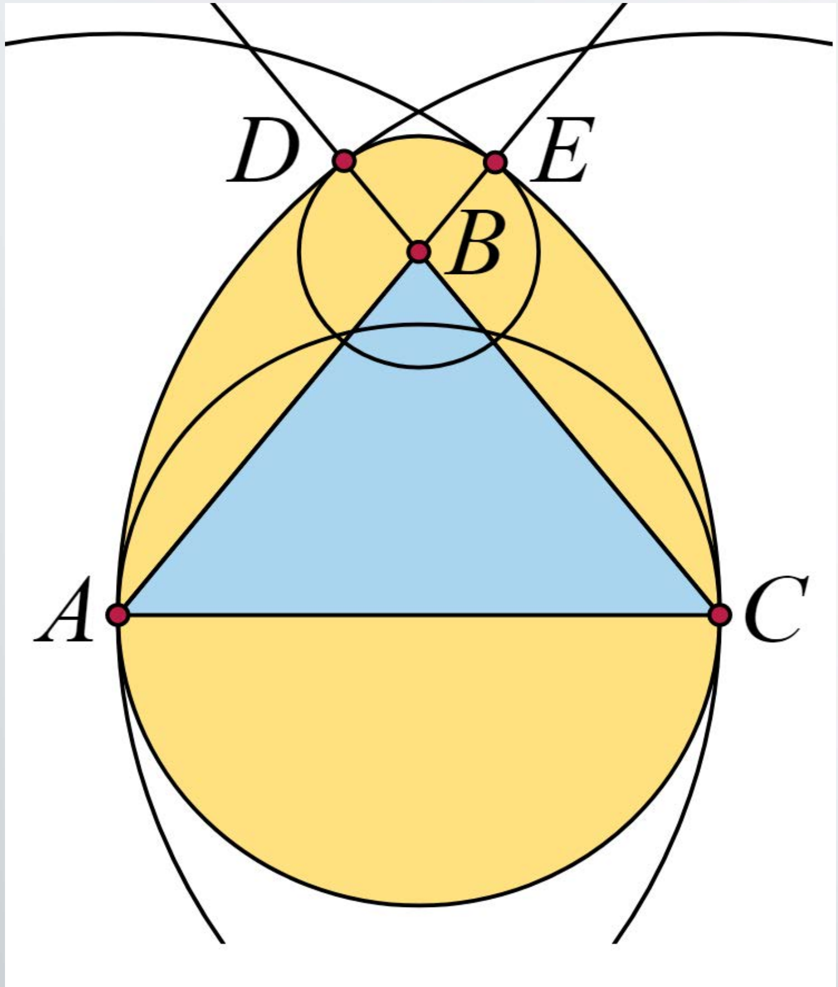

Figure 3. Moss's Euclidean egg geometry used for the design of medium (53-62 g) , large (63-72 g) and extra large (>72 g) eggs.

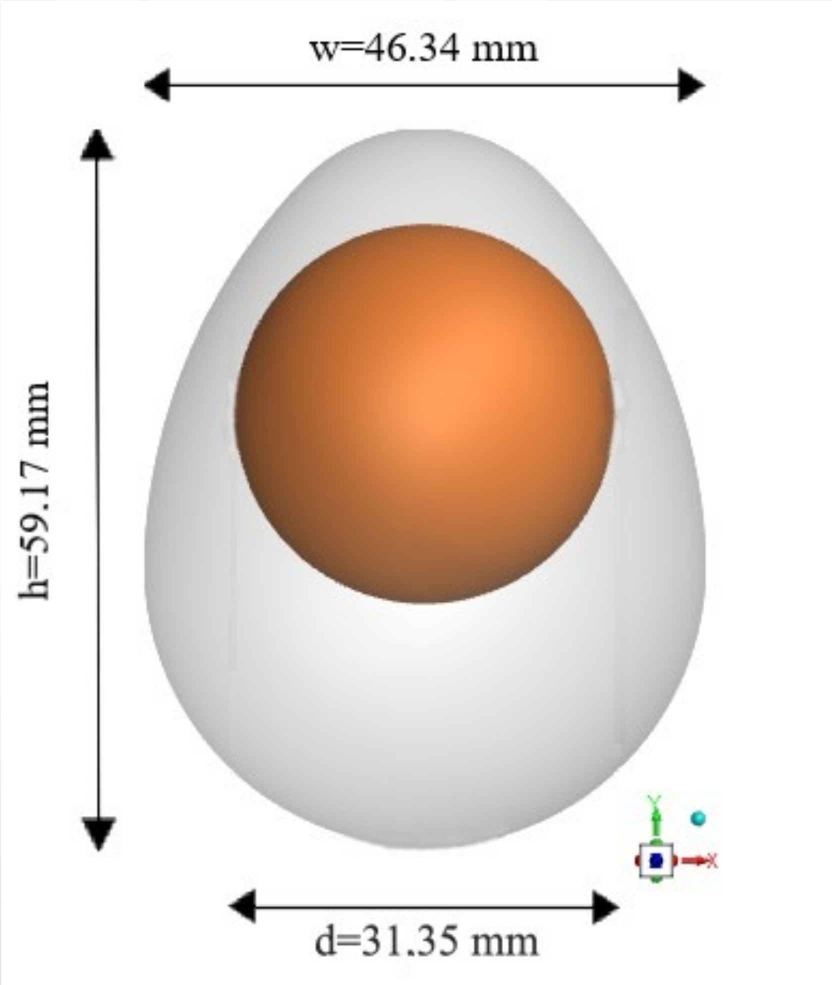

Figure 4. Shape and dimensions for the large size egg used for the simulations.

CFD model mesh

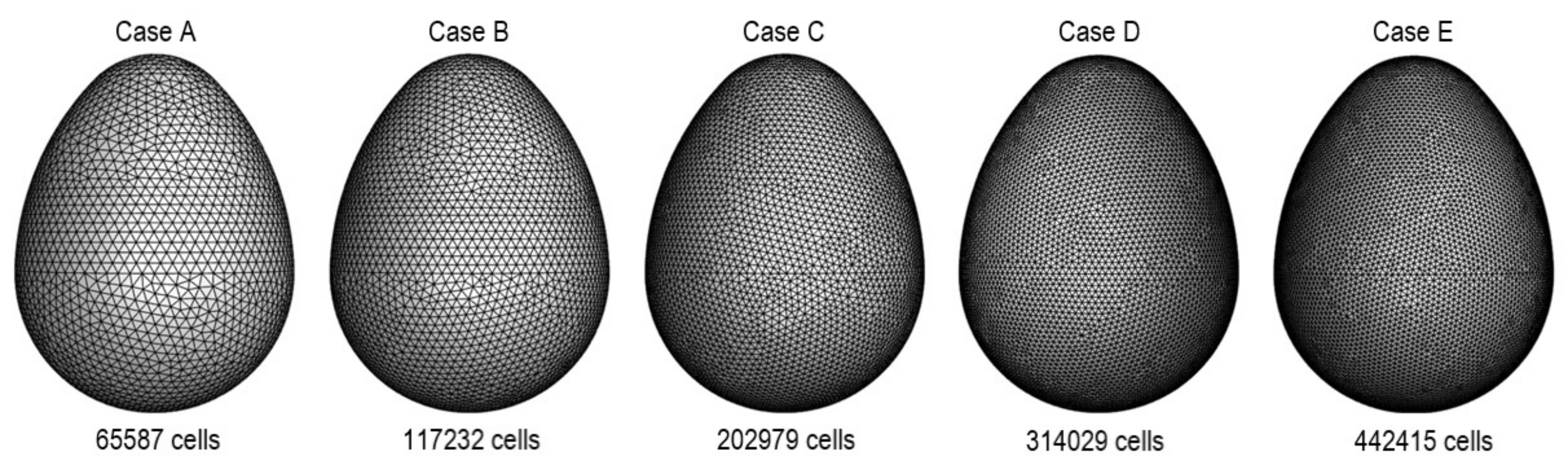

Figure 5. Illustration of the 5 meshes constructed in the Meshing program.

Mesh independence

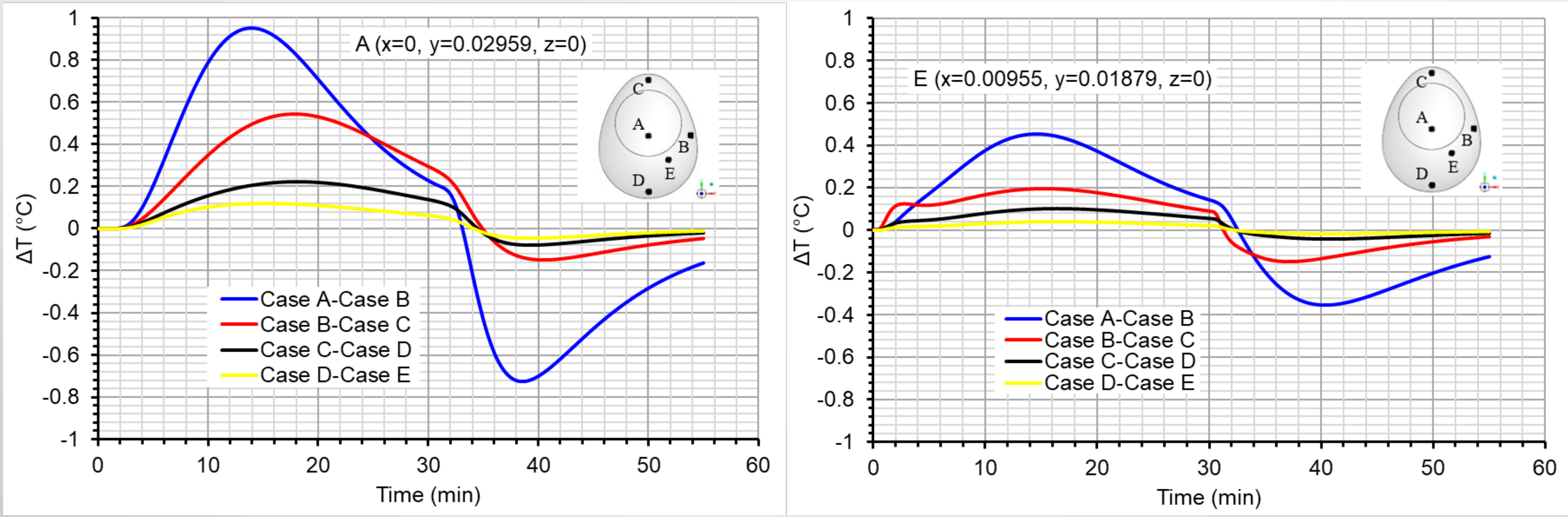

Figure 6. Comparison, at points A and E, of the five meshes examined, from lower to higher density, for T_{IT}=20°C, T_{RT}=58°C and T_{CW}=20°C.

Initial and boundary conditions

- The external surface of the geometry represents the eggshell was defined as wall
- The internal volume of both the yolk and the albumen was defined as fluid
- A constant temperature condition was applied to the external surface of the egg (54 °C, 56 °C, 58 °C, 60 °C)
- The initial temperature of the egg was 20 °C
- The gravitational force was set to g=9.81 (m/s^2)
- The constant time step was 1 s
- The convergence criterion was set to $1*10^{-6}$

Thermophysical properties

Table 1. Thermophysical properties of the various egg components used for the CFD.

Property (units)	Egg component	Value/ Equation
Density (r) (kg/m^3)	Egg white	1048
	Yolk	1035
	Shell	2300
Specific heat (C_p) (J/kg·K)	Egg white	3560
	Yolk	3560
	Shell	888
Thermal conductivity (k) (W/m·K)	Egg white	$0.43+0.00055 \cdot T$
	Yolk	0.337
	Shell	2.25
Viscosity (m) (Kg/m·s)	Egg white	$3.12-0.0089 \cdot T$
	Yolk	$1.60-0.0048 \cdot T$
	Shell	-

T in Kelvin.

Convective heat transfer coefficient

- The temperature was monitored at the center of the aluminum sphere.

- Convective heat transfer coefficient, h, was calculated from the slope of the $\ln(\frac{T-T_\infty}{T_{IT}-T_\infty})$ vs t straight line, fitted to the experimental data

- The experiments were performed in duplicate for both heating and cooling

- For heating medium h_h=640 W/(m^{2}K) and for cooling medium h_c=1290 W/(m^{2}K).

Figure 7. Aluminum sphere used, along with the thermocouple used for temperature monitoring.

Convective heat transfer coefficient

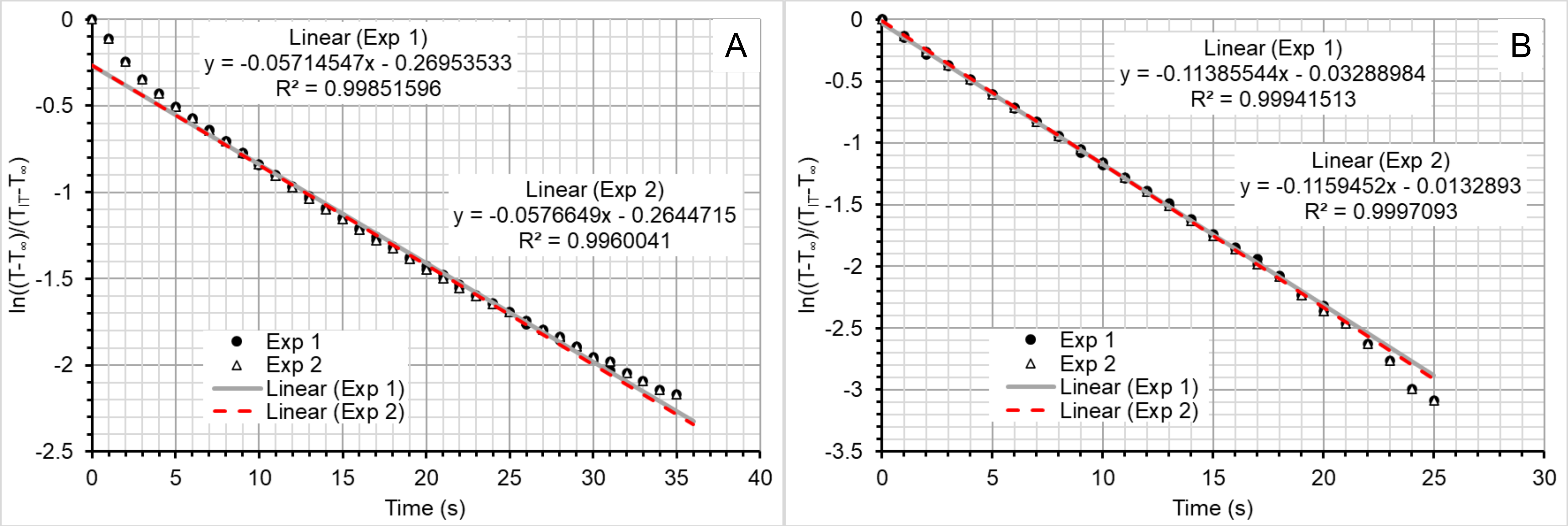

Figure 8. Determination of the convective heat transfer coefficients between the heating (A) and the cooling (B) medium and the egg surface (from two experiments, Exp 1 and Exp 2, for each case).

Validation experiments

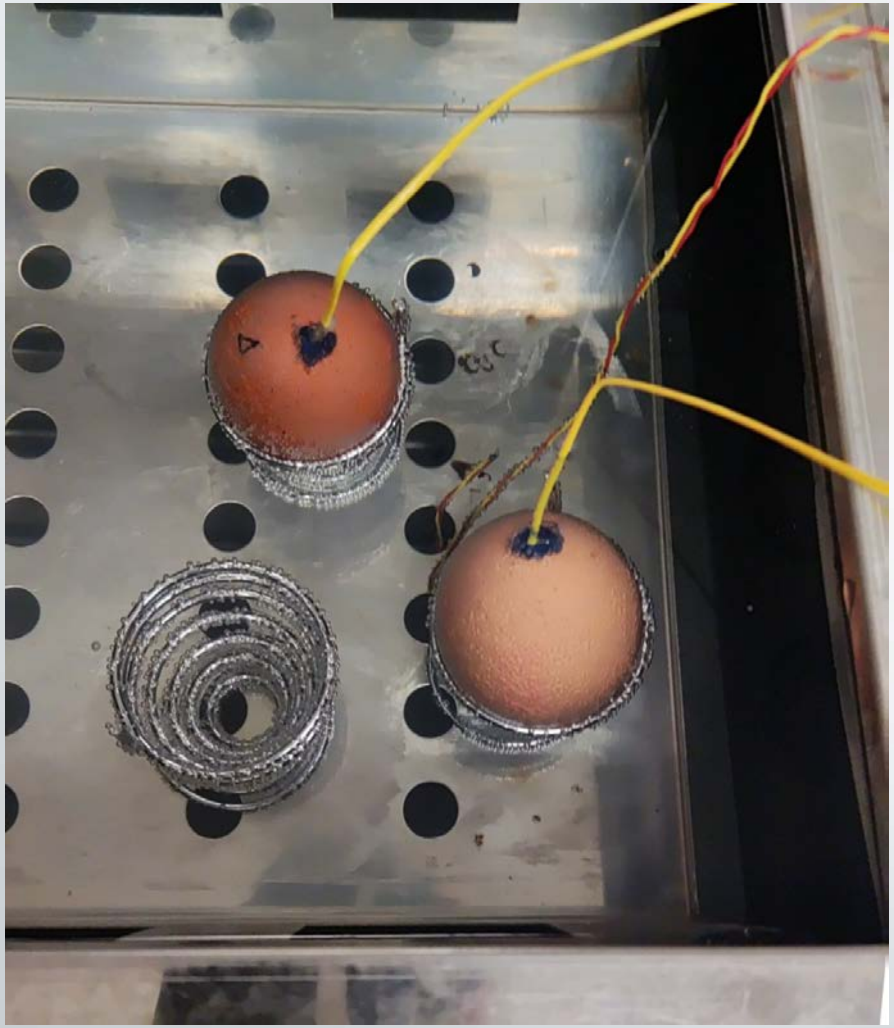

Figure 9. Eggs in water-bath during heating process.

Figure 10. Determination of thermocouple position.

Thermal process calculations

Salmonella enteritidis: $D_{60°C}$ = 0.17 min, z = 4.1°C

Time required for 5 log reduction at 60°C: 0.85 min

F value calculations (based on CFD time temperature data)

$$F_{T_{ref}}^{z} = D_{T_{ref}}\left[\log(C_a) - \log(C_b)\right] = \int_{t=0}^{t=t_{emd}} 10^{\frac{T-T_{ref}}{z}} dt$$

Heating time, *B*, calculations (through a trial-and-error procedure)

$$F_{T_{ref}}^{z} = \int_{t_h=0}^{t_h=B} 10^{\frac{T-T_{ref}}{z}} dt_h + \int_{t_c=0}^{t_c=t_{end}} 10^{\frac{T-T_{ref}}{z}} dt_c$$

Thermal process calculations

Quality retention calculations (*F* value equation solved for C/C_o)

$$\frac{C}{C_o} \times 100 = 10^{-\frac{\int_{t=0}^{t=t_p} 10^{\frac{T(t)-T_{ref}}{z}} dt}{D_{T_{ref}}}} \times 100$$

Quality calculations were based on general thermal inactivation kinetic parameters reported for quality attributes.

Results and Discussion

Validation experiments

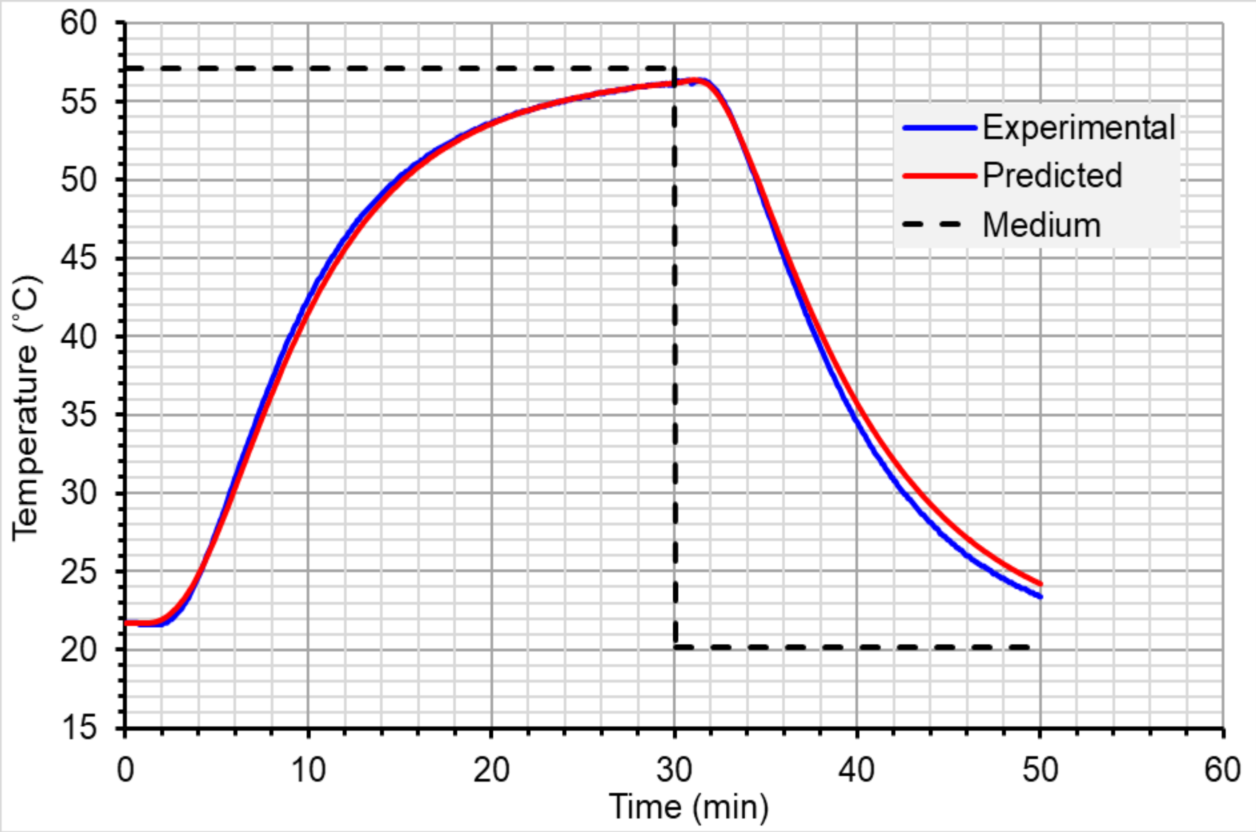

Figure 11. Comparison between predicted and experimental temperature evolution data during heating and cooling of large size egg.

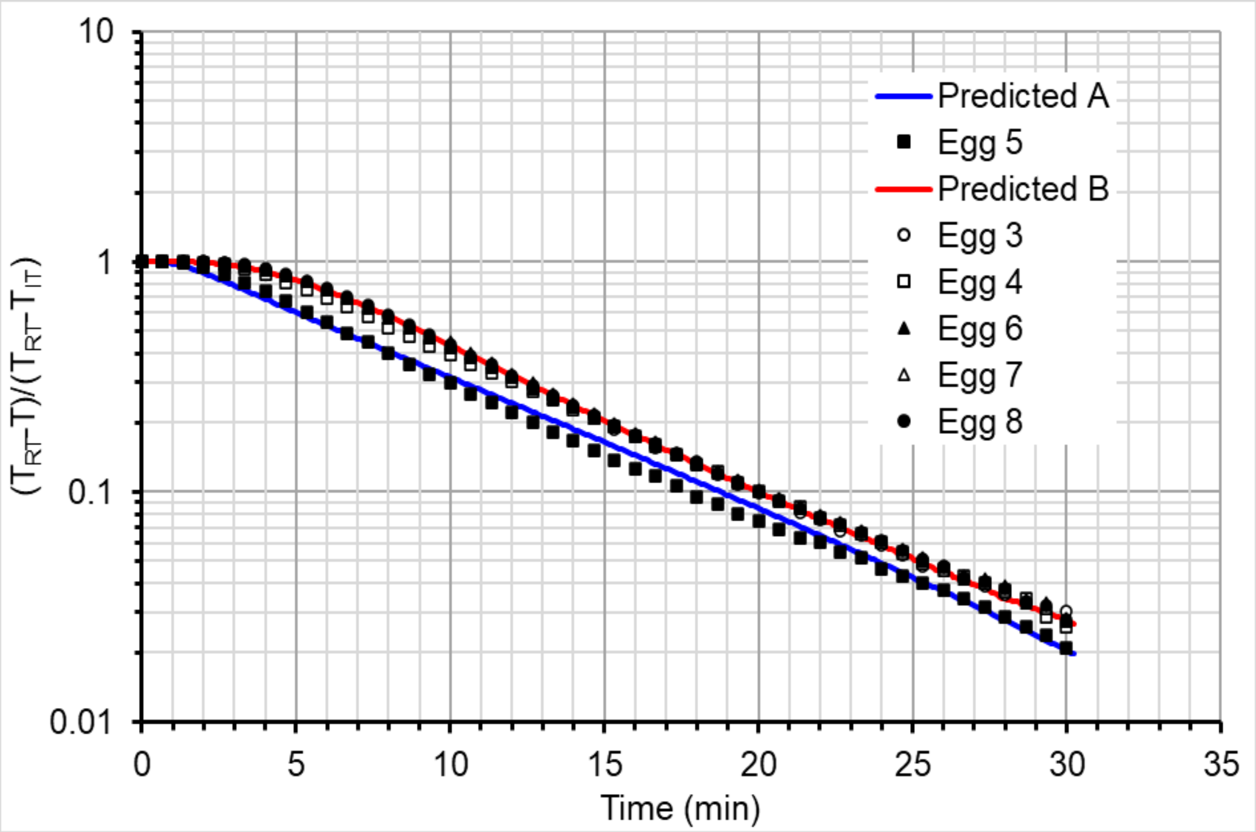

Figure 12. Comparison between predicted and experimental unaccomplished temperature ratios at different positions, A and B, at the egg interior during heating of individual large size eggs.

Thermal process calculations

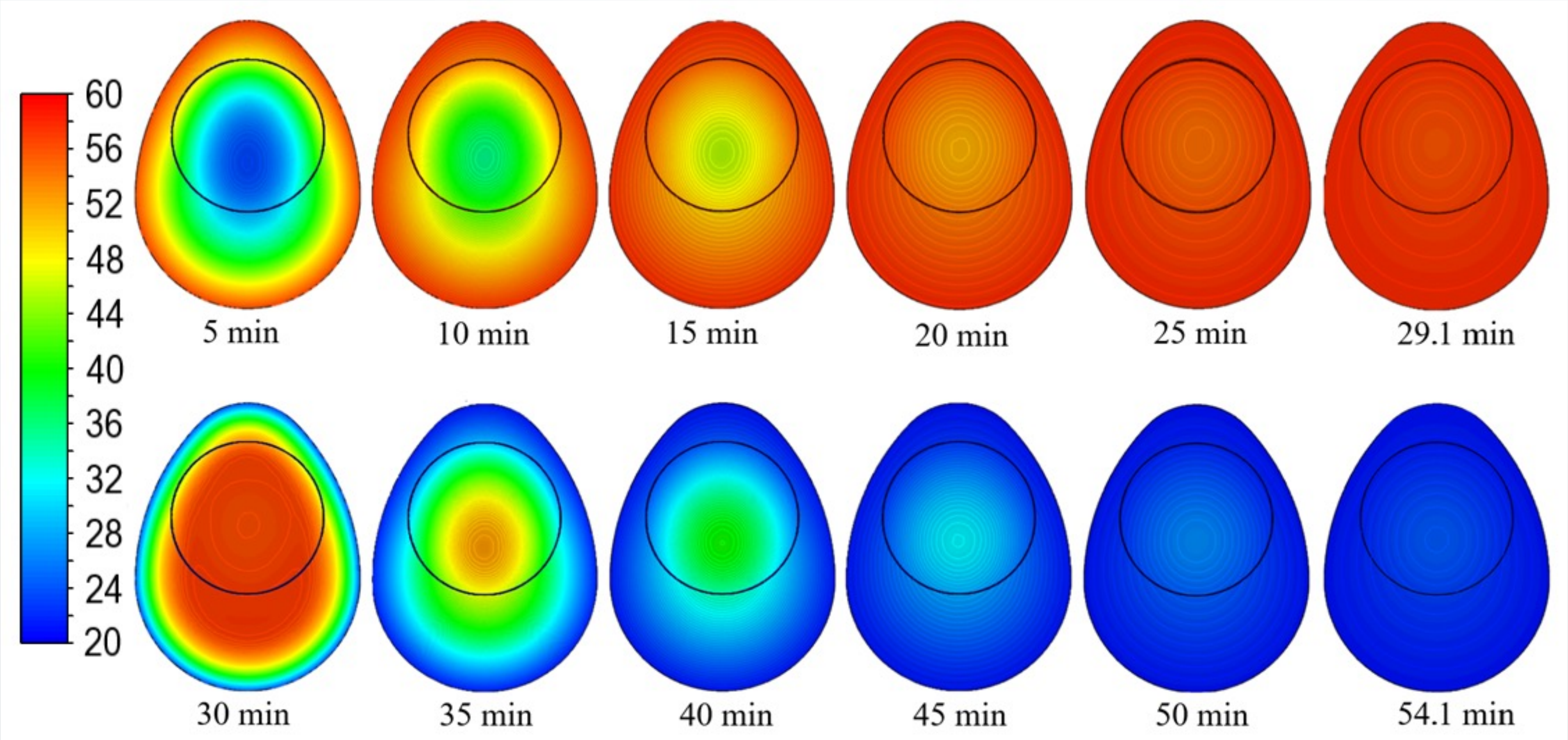

Figure 13. Evolution of temperature distribution (°C), vertical cross section, for the large size egg during 29.1 min of heating at 58°C and 25.0 min of cooling at 20°C.

Thermal process calculations

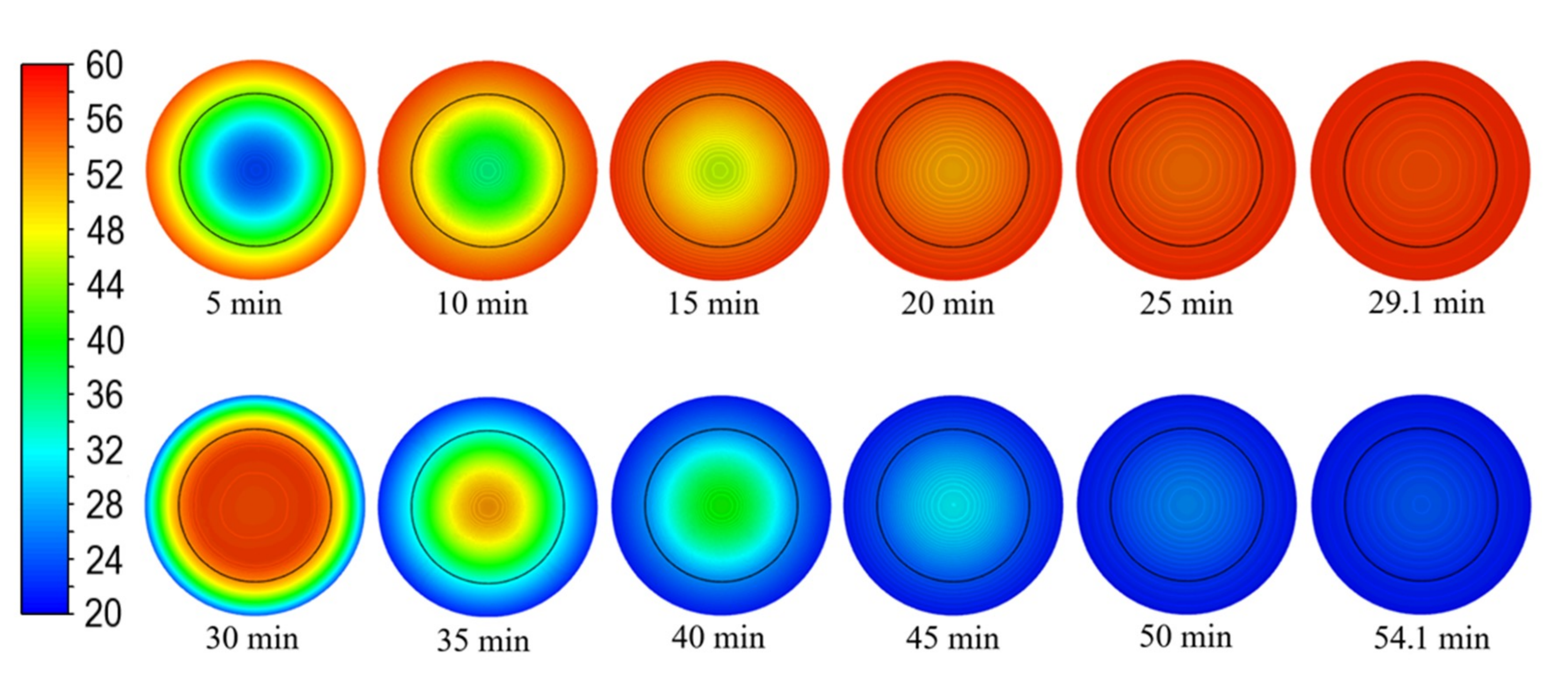

Figure 14. Evolution of temperature distribution (°C), horizontal cross section, for the large size egg during 29.1 min of heating at 58°C and 25.0 min of cooling at 20°C.

Thermal process calculations

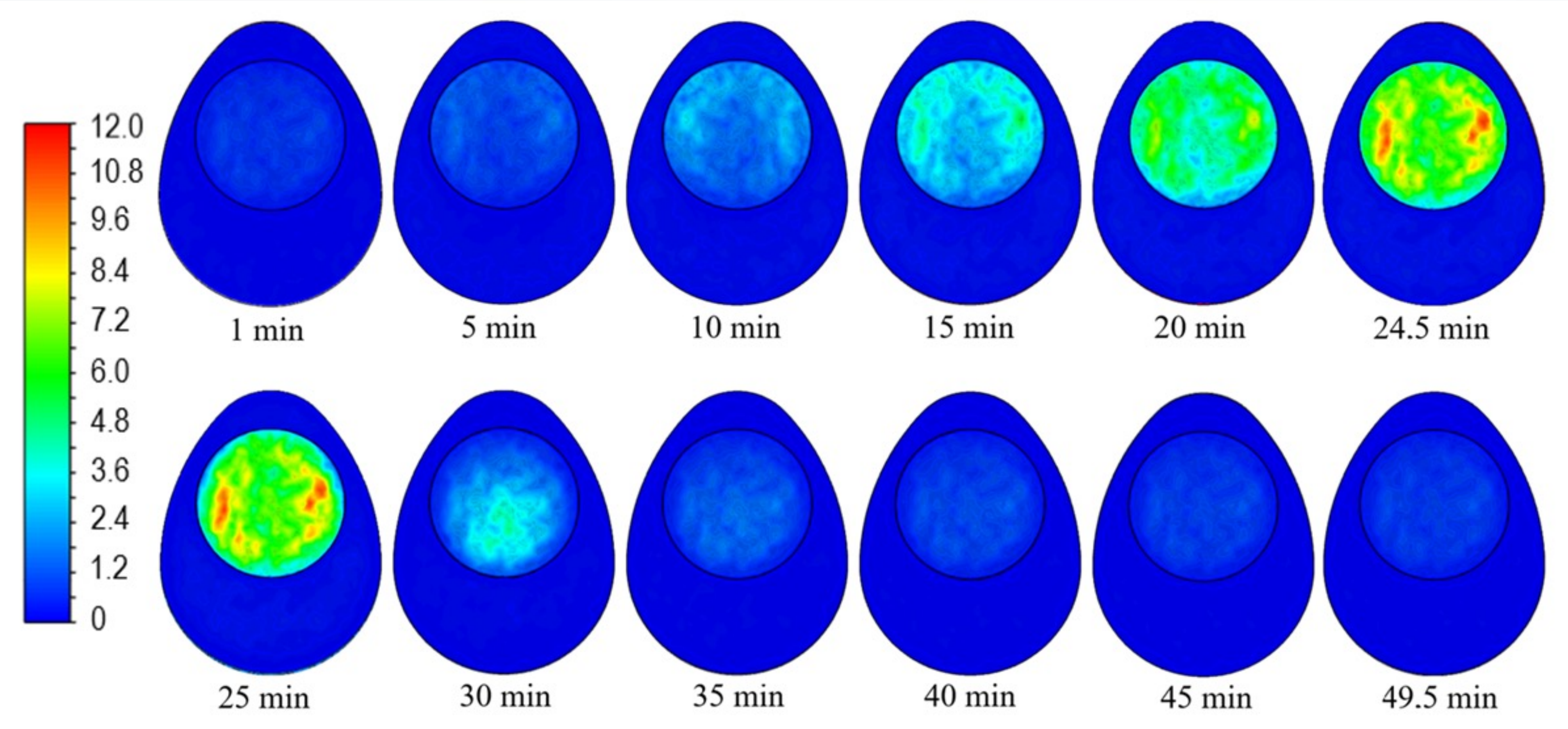

Figure 17. Evolution of velocity, in $10^{-5}\times$ m/s, distribution, horizontal cross section, for the large size egg during 24.5 min of heating at 60°C and 25.0 min of cooling at 20°C.

Thermal process calculations

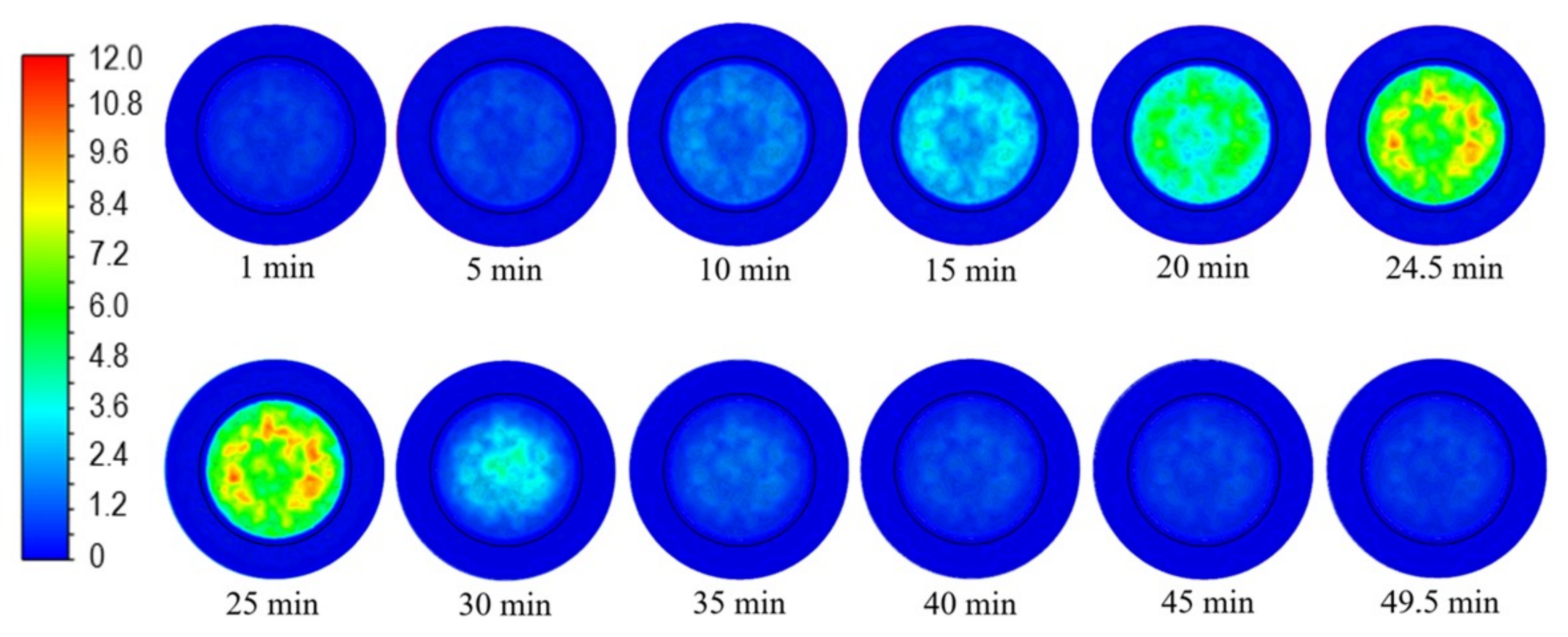

Figure 18. Evolution of velocity, in $10^{-5}\times$ m/s, distribution, vertical cross section, for the large size egg during 24.5 min of heating at 60°C and 25.0 min of cooling at 20°C.

Thermal process calculations

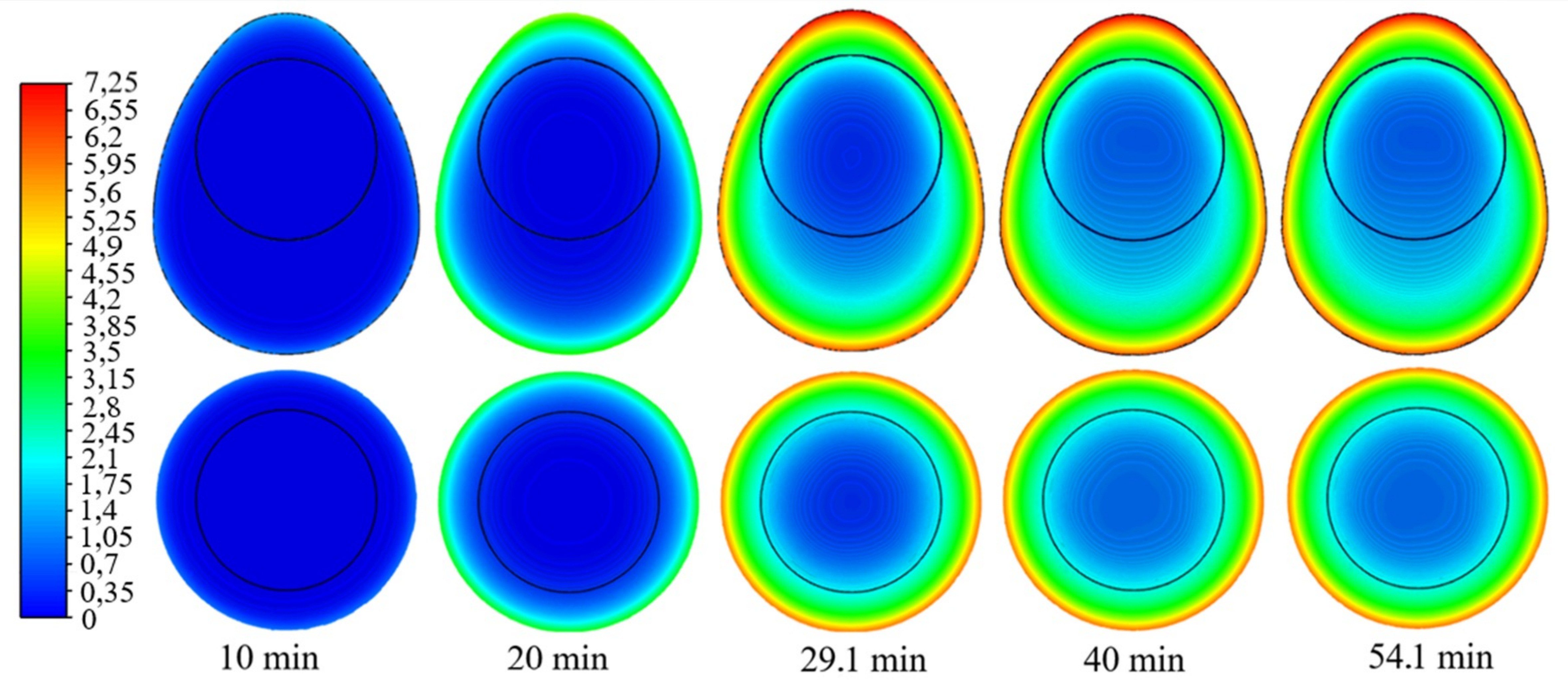

Figure 19. Evolution of the *F* value (min) distribution, horizontal and vertical cross sections, for the large size egg during 29.1 min of heating at 58°C and 25.0 min of cooling at 20°C.

Thermal process calculations

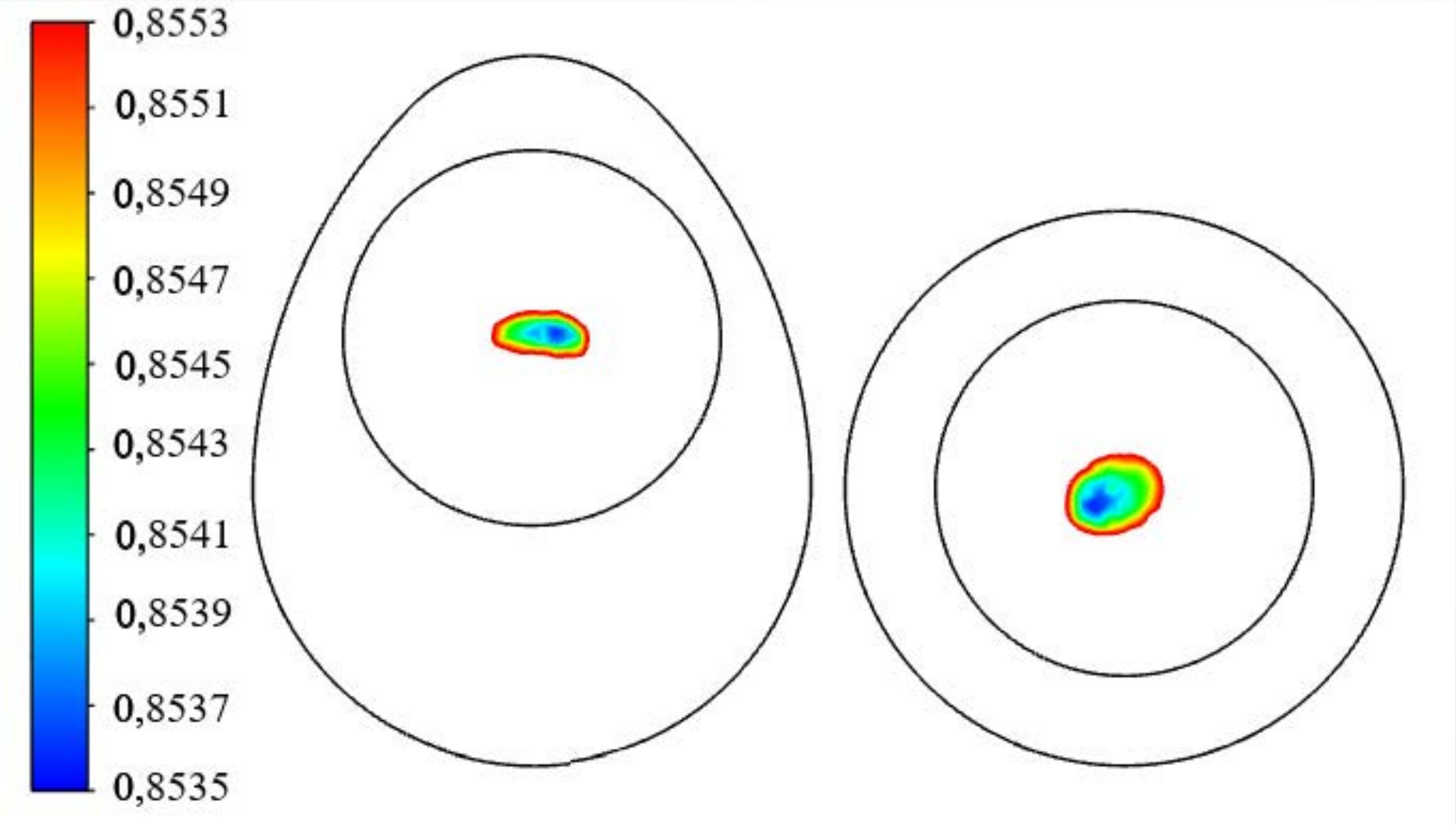

Figure 20. Determination of the critical point at the end of the pasteurization process, i.e., for $F_{60°C}^{4.1°C}$=0.85 min, for the large size egg during 29.1 min of heating at 58°C and 25.0 min of cooling at 20°C.

Thermal process calculations

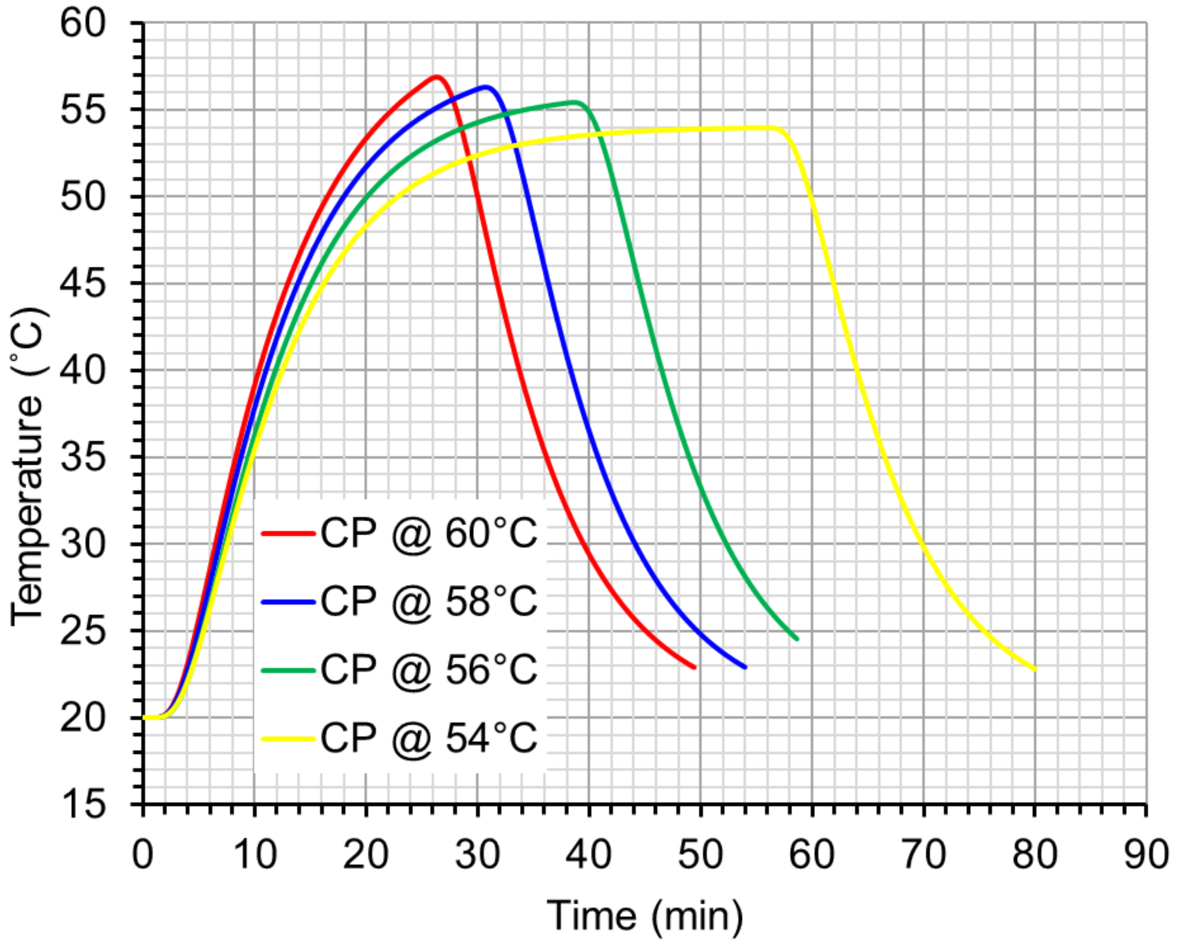

Figure 15. Temperature evolution at the critical point (CP) during large size egg pasteurization, for processes targeting $F_{60°C}^{4.1°C}$=0.85 min at different medium temperatures.

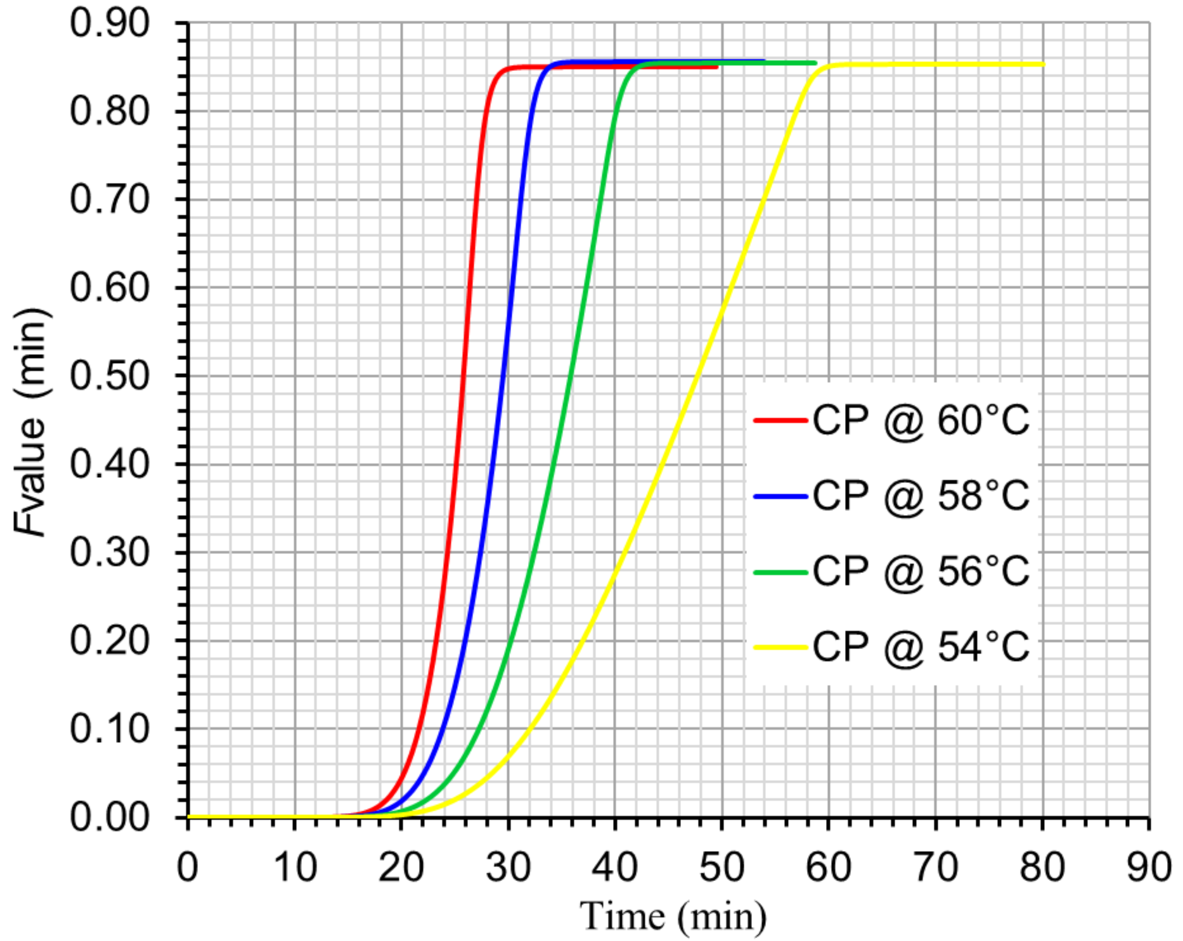

Figure 16. $F_{60°C}^{4.1°C}$ value evolution at the critical point (CP) during large size egg pasteurization, for processes targeting $F_{60°C}^{4.1°C}$=0.85 min at different medium temperatures.

Required heating times

Table 3. Required heating times, *B*, for a target $F_{60°C}^{4,1°C}$ value of 0.85 min, together with the $F_{heating}$ and $F_{cooling}$ values, during egg pasteurization at different time and temperature conditions.

Egg size	Heating medium *T* (°C)	Heating time *B* (min)	F_{total}	$F_{heating}$	$F_{cooling}$	% contribution of cooling lethality
Medium	58	26.3	0.86	0.49	0.37	43.0%
Large	54	55.1	0.85	0.74	0.11	13.0%
	56	37.2	0.86	0.60	0.26	29.9%
	58	29.1	0.86	0.46	0.40	46.2%
	60	24.5	0.86	0.32	0.53	62.3%
Extra Large	58	28.7	0.85	0.37	0.48	56.5%

Retention of quality attributes

Table 2. Retention of quality attributes, characterized by different *D* and *z* values, during large size egg pasteurization at different time and temperature conditions.

Heating medium *T* (°C)	Heating time *B* (min)	$D_{121,11°C}$ (min)	z (°C)	$D_{121,11°C}$ (min)	z (°C)	$D_{121,11°C}$ (min)	z (°C)	$D_{121,11°C}$ (min)	z (°C)
		100	20	1000	20	100	50	1000	50
54	55.1	99.95		100.00		94.22		99.41	
56	37.2	99.96		100.00		95.77		99.57	
58	29.1	99.97		100.00		96.34		99.63	
60	24.5	99.97		100.00		96.67		99.66	

Conclusion

- The required heating times at different heating medium temperatures were estimated
- Microbial destruction during cooling ranged between 13.0% and 62.3% of the total destruction
- The higher the heating medium temperature, the higher the contribution of the cooling cycle to the total lethality
- Ignoring the lethality during the cooling cycle can lead to unnecessary long heating times
- Finally, quality degradation seems minimal during the thermal pasteurization

Thank You

For Your Attention